



Pleistocene vertical carbon isotope and carbonate gradients in the South Atlantic sector of the Southern Ocean

David A. Hodell and Kathryn A. Venz

Department of Geological Sciences, University of Florida, Gainesville, Florida 32611, USA (dhodell@geology.ufl.edu; venz@ufl.edu)

Christopher D. Charles

Geosciences Research Division, Scripps Institution of Oceanography, University of California, San Diego, La Jolla, California 92093, USA (ccharles@ucsd.edu)

Ulysses S. Ninnemann

Geosciences Research Division, Scripps Institution of Oceanography, University of California, San Diego, La Jolla, California 92093, USA

*Now at Geologisk Institutt, Universitetet I Bergen, Allegaten 41, N-5007 Bergen, Norway.
(ulysses.ninnemann@geol.uib.no)*

[1] We demonstrate that the carbon isotopic signal of mid-depth waters evolved differently from deep waters in the South Atlantic sector of the Southern Ocean during the Pleistocene. Deep sites (>3700 m) exhibit large glacial-to-interglacial variations in benthic $\delta^{13}\text{C}$, whereas the amplitude of the $\delta^{13}\text{C}$ signal at Site 1088 (~2100 m water depth) is small. Unlike the deep sites, at no time during the Pleistocene were benthic $\delta^{13}\text{C}$ values at Site 1088 lower than those of the deep Pacific. Reconstruction of intermediate-to-deep $\delta^{13}\text{C}$ gradients ($\Delta^{13}\text{C}_{\text{I-D}}$) supports the existence of a sharp chemocline between 2100 and 2700 m during most glacial stages of the last 1.1 myr. This chemical divide in the glacial Southern Ocean separated well-ventilated water above ~2500 m from poorly ventilated water below. The $\Delta^{13}\text{C}_{\text{I-D}}$ signal parallels the Vostok atmospheric pCO_2 record for the last 400 kyr, lending support to physical models that invoke changes in Southern Ocean deep water ventilation as a mechanism for changing atmospheric pCO_2 . The emergence of a strong 100-kyr cycle in $\Delta^{13}\text{C}_{\text{I-D}}$ during the mid-Pleistocene supports a change in vertical fractionation and deep-water ventilation rates in the Southern Ocean, and is consistent with possible CO_2 -forcing of this climate transition.

Components: 7562 words, 14 figures, 2 tables.

Keywords: Carbon isotopes; carbonate; Pleistocene; southern ocean; deep water circulation; carbon dioxide.

Index Terms: 4267 Oceanography: General: Paleooceanography; 4806 Oceanography: Biological and Chemical: Carbon cycling; 1030 Geochemistry: Geochemical cycles (0330); 1050 Geochemistry: Marine geochemistry (4835, 4850).

Received 19 April 2002; **Revised** 30 July 2002; **Accepted** 1 August 2002; **Published** 10 January 2003.

Hodell, D. A., K. A. Venz, C. D. Charles, and U. S. Ninnemann, Pleistocene vertical carbon isotope and carbonate gradients in the South Atlantic sector of the Southern Ocean, *Geochem. Geophys. Geosyst.*, 4(1), 1004, doi:10.1029/2002GC000367, 2003.



1. Introduction

[2] It has long been recognized that the vertical distribution of nutrients and carbon in the ocean is an important aspect of the global carbon cycle on geological timescales. *Boyle* [1988] first proposed a mechanism for changing atmospheric $p\text{CO}_2$ whereby nutrients and metabolic CO_2 are shifted from intermediate to deep water during glacial periods of the late Pleistocene. Increased CO_2 lowers the deep ocean carbonate ion concentration and increases dissolution in the deep sea. This triggers an alkalinity response as increased dissolution in the deep ocean is compensated for by a drop in the carbonate compensation depth (CCD). Atmospheric CO_2 decreases accordingly, but lags oceanographic forcing because it takes thousands of years for the carbonate system to respond to changes in vertical chemical gradients.

[3] More recently, *Toggweiler* [1999] proposed a variation on Boyle's "vertical fractionation" concept that does not include changes in biological production or nutrient distribution. Similar to *Boyle* [1988], the model considers the boundary between intermediate and deep water as a chemical divide that separates low CO_2 water above from high CO_2 water below. Unlike *Boyle* [1988], however, the high CO_2 below the divide is caused by reduced ventilation of bottom water creating strongly depleted $\delta^{13}\text{C}$ values without an attendant change in nutrient concentrations. Atmospheric $p\text{CO}_2$ reduction in *Toggweiler's* model results from the combined effects of decreased ventilation (21 ppm) and a carbonate alkalinity response (36 ppm).

[4] If they are to be tested, vertical fractionation models require a global array of depth transects that reconstruct past intermediate-to-deep chemical gradients. For example, reconstruction of Cd/Ca and $\delta^{13}\text{C}$ of benthic foraminifers with depth in the North Atlantic has provided crucial evidence for a shift of nutrients from intermediate to deep waters during the last glacial period [*Boyle*, 1992; *Oppo and Lehman*, 1993] as North Atlantic Deep Water (NADW) was converted to an intermediate water mass (Glacial North Atlantic Intermediate Water or upper NADW). Similar depth transects in the Pacific and Indian Oceans have also found sharp

$\delta^{13}\text{C}$ gradients at ~ 2000 m water depth during glacial periods [*Mix et al.*, 1991; *Herguera et al.*, 1992; *McCorkle et al.*, 1998; *Matsumoto et al.*, 2002].

[5] Few studies of vertical chemical gradients have been undertaken in the Southern Ocean for a variety of reasons including: (1) a general lack of suitable topographic rises for depth transects; (2) in some areas, a shallow local lysocline discourages carbonate preservation; and (3) the widespread dominance of biosiliceous sediment during glaciations renders benthic foraminifera scarce. Most studies have focused on $\delta^{13}\text{C}$ comparisons between the last glacial maximum (LGM) and Holocene [*Lynch-Stieglitz et al.*, 1994; *Ninnemann and Charles*, 1997, 2002; *Matsumoto and Lynch-Stieglitz*, 1999], and few reconstructions have included sites from intermediate water depths. Here we present records of vertical $\delta^{13}\text{C}$ and carbonate gradients along a depth transect down the northern flank of the Agulhas Ridge in the South Atlantic Ocean. The Pleistocene records of intermediate-to-deep $\Delta^{13}\text{C}$ and carbonate dissolution are used to evaluate whether glacial-to-interglacial changes in vertical chemical gradients in the Southern Ocean were important for influencing atmospheric $p\text{CO}_2$ variation.

2. Site Locations

[6] Ocean Drilling Program (ODP) Leg 177 drilled three sites (Sites 1088, 1089 and 1090) in the northern Subantarctic Zone of the South Atlantic between $\sim 41^\circ$ and 43°S (Figure 1), which form a depth transect down the northern flank of the Agulhas Ridge (Figure 2). The sites span water depths from 2082 to 4620 m, but are separated by less than 2° of latitude (Table 1). As such, they are in essentially the same surface water mass and, therefore, we expect similar surface water variability (planktic isotopic signals) among sites.

[7] Site 1088 (2082 m) was drilled on the northeastern part of the Agulhas Ridge where it is a broad and relatively shallow topographic feature (Figure 2). The site is near the interface of upper North Atlantic Deep Water (NADW) and upper Circumpolar Deep Water (CDW) (Figure 3). Site

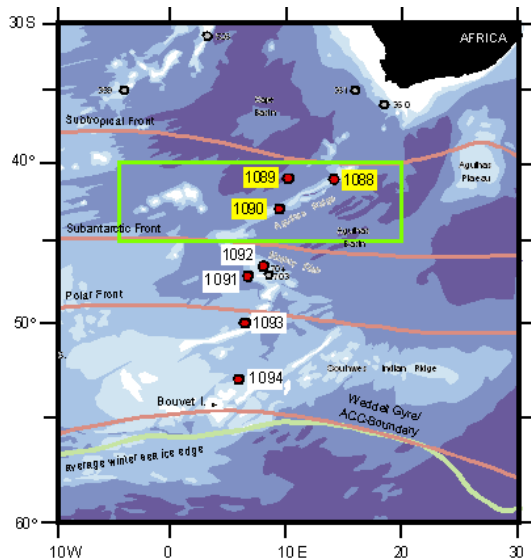


Figure 1. Location of sites drilled during ODP Leg 177. Details of boxed area are shown in Figure 2 [after *Shipboard Scientific Party, 1999*].

1090 (3702 m) and its associated piston core (TTN057-6) are positioned on the southwest portion of the ridge, where the Agulhas Ridge narrows considerably and the topography steepens. Site 1090 was mistakenly reported as located on the southern flank of the ridge in the Leg 177 Initial Reports [*Gersonde et al., 1999*] when, in fact, it is on the northern flank of the Agulhas Ridge in the southernmost Cape Basin (Figure 2). Piston core TTN057-6 was retrieved as part of the site survey for ODP Leg 177, and is located very close to Site 1090 (Table 1). Both sites are in ~3700 m of water

and near the interface of lower NADW and lower CDW (Figure 3). Site 1089 (4620 m) was drilled on a sediment drift in the southern Cape Basin close to the northern flank of the Agulhas Ridge and it is bathed by nearly pure lower CDW (Figures 2 and 3).

[8] Sedimentation rates among sites vary by an order of magnitude. Site 1088 has the lowest sedimentation rates (averaging 1 cm/1000 yr), yet all marine isotope stages (MIS) between 1 and 31 are identifiable in the record (Figure 4a) [*Hodell et al., 2002*]. Piston core TTN057-6 and Site 1090 have average sedimentation rates of 3 cm/1000 yr in the Pleistocene [*Hodell et al., 2000; Venz and Hodell, 2002*]. Site 1089 is located on a sediment drift and has sedimentation rates averaging 15 cm/1000 yr for the past 600 kyrs [*Shipboard Scientific Party, 1999; Wildeboer Shut et al., 2002*].

3. Methods

[9] At Site 1088, we sampled the upper 13.2 m of sediment in Hole 1088B (Cores 1088B-1H and 1088B-2H) at a spacing of one sample every 5 cm. The benthic foraminifer *Cibicidoides wuellerstorfi* was picked from the >150 μm size fraction and specimens of the planktic foraminifer *Globigerina bulloides* were selected from the >212 to <300 μm size fraction for stable isotope analysis.

[10] The “Site 1090” record represents a hybrid of isotope results from piston core TTN057-6-PC4

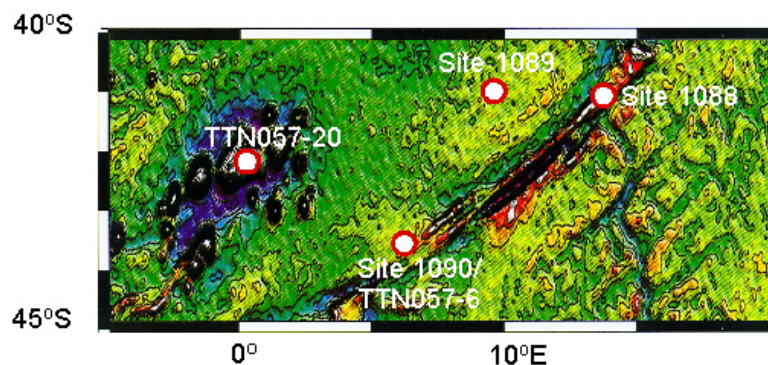


Figure 2. Gravity field of the southernmost Cape Basin and northernmost Agulhas Basin in the South Atlantic. The NE-SW trending feature is the Agulhas Fracture Zone Ridge and the shallow feature to the west is Discovery Seamount. Site locations are shown for cores taken aboard the R/V *Thomas G. Thompson* Cruise TTN057 and ODP Leg 177.



Table 1. Location, Water Depth, and Physical Properties of the Water Masses at the Sites Comprising the Agulhas Ridge Transect

	Latitude	Longitude	Depth, m	Pot. T, °C	Salinity	Density, σ_t
ODP Site 1088	41°8.163'S	13°33.77'E	2082	2.43	34.749	27.7214
ODP Site 1090	42°54.82'S	8°53.98'E	3702	1.11	34.723	27.7951
TTN057-6-PC4	42°52.40'S	8°58.40'E	3751	1.05	34.719	27.7952
ODP Site 1089	40°56.19'S	9°53.65'E	4621	0.62	34.684	27.7908

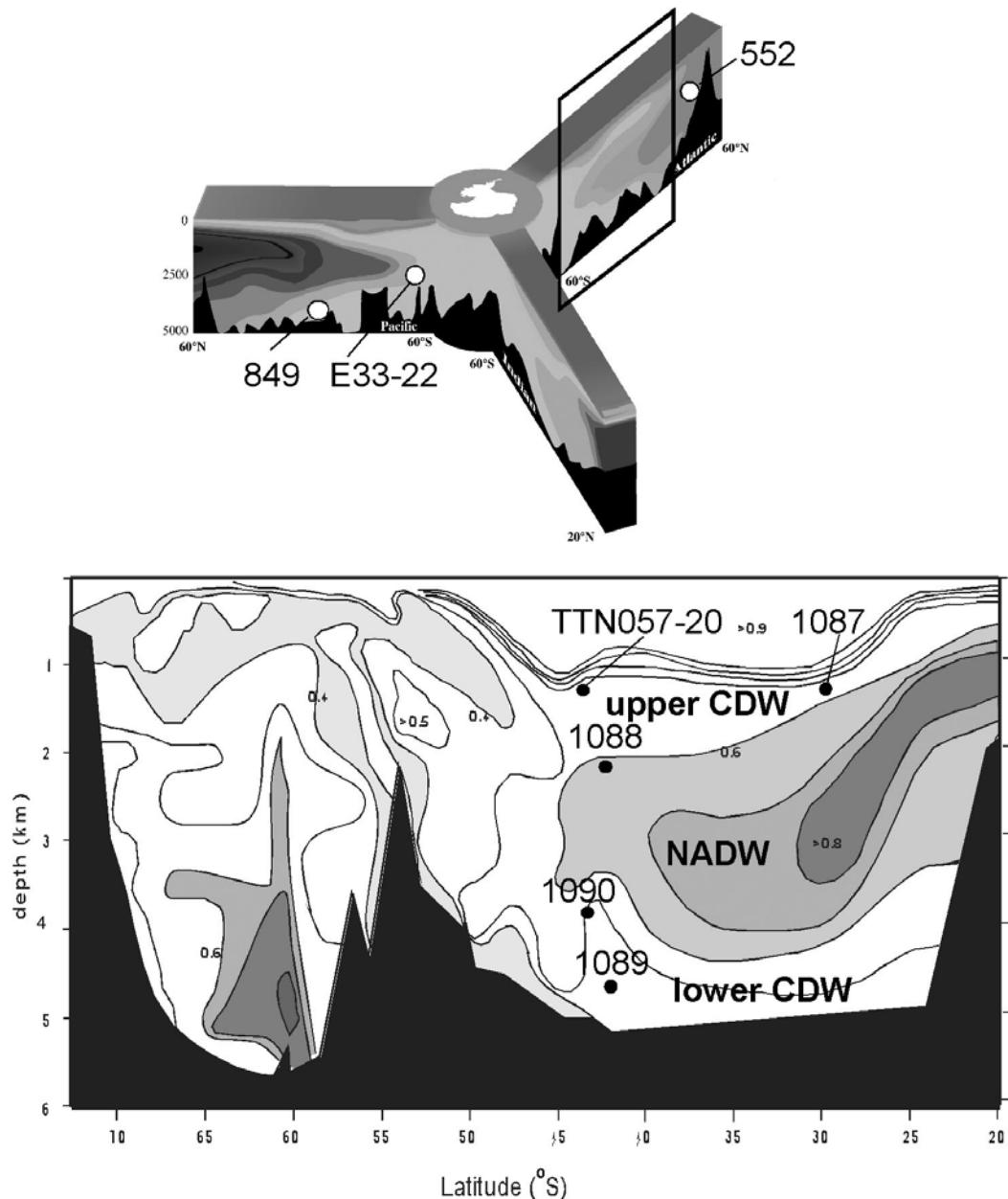


Figure 3. (a) Vertical distribution of $\delta^{13}\text{C}$ of DIC in the world's oceans (data from *Kroopnick* [1985]; figure modified after *Charles and Fairbanks* [1990]) relative to the core locations used in this study. (b) Enlargement of the South Atlantic part of the contoured $\delta^{13}\text{C}$ DIC map showing the position of the South Atlantic piston and ODP cores discussed in the text. Figure modified after *Ninnemann and Charles* [2002].

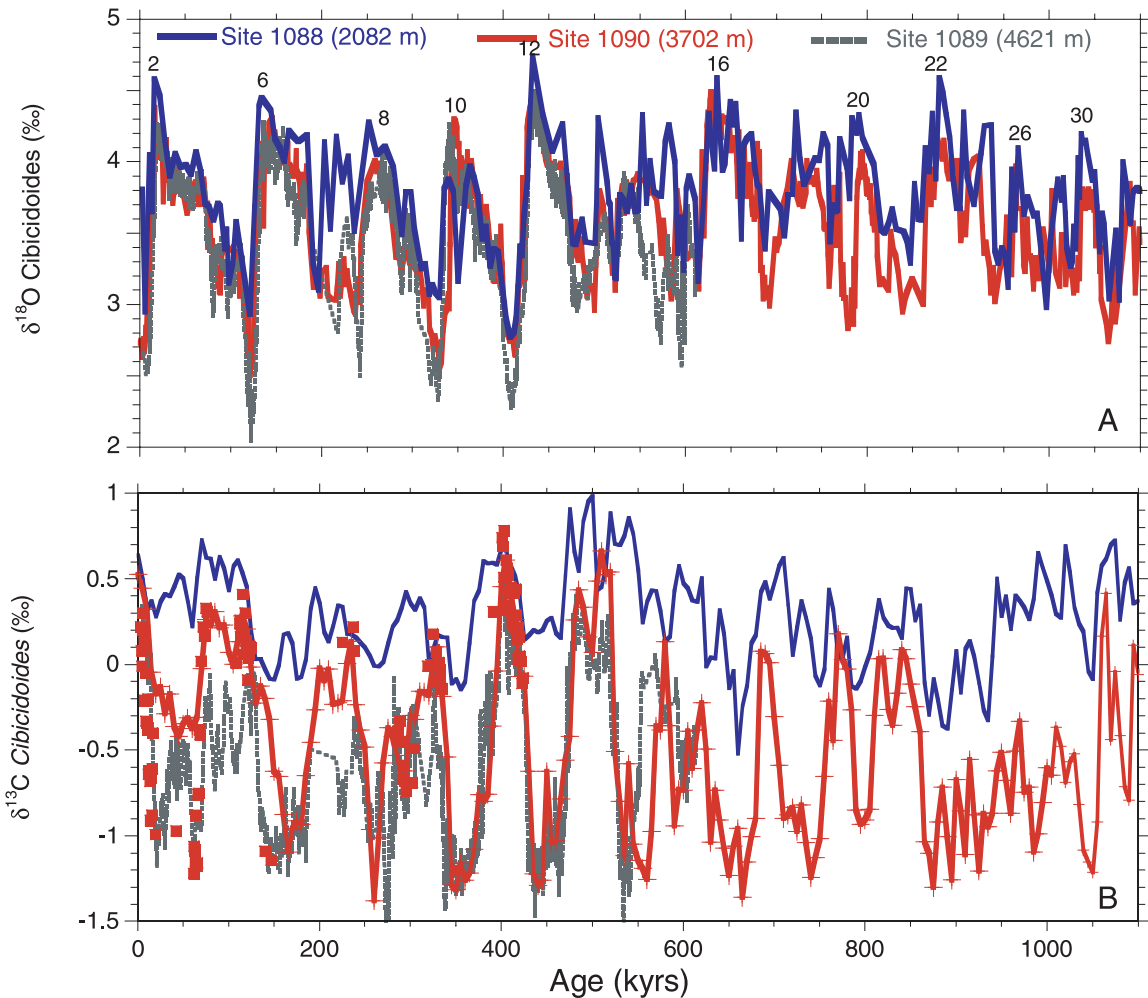


Figure 4. (a) Benthic oxygen isotopic records of ODP Sites 1088 (blue), 1090 (red), and 1089 (gray) with marine isotope stages designated. (b) Benthic carbon isotopic records of ODP Sites 1088 (*C. wuellerstorfi*), 1090 (*C. wuellerstorfi*), and 1089 (*Cibicidoides* spp.). Filled red squares represent analyses of *C. kullenbergi* at Site 1090. All carbon isotope records (except for *C. kullenbergi* at Site 1090) were interpolated to a constant time interval of 5 kyrs, corresponding to the sampling resolution of Site 1088, which has the lowest sedimentation rate.

[Hodell *et al.*, 2000] and Site 1090 [Venz and Hodell, 2002]. The two records were spliced at ~12.1 mcd (~400 kyr). Stable isotopes were measured separately on specimens of *Cibicidoides wuellerstorfi* and *Cibicidoides kullenbergi* in some samples. *G. bulloides* was measured from the >212 to <300 μm size fraction.

[11] At site 1089, mixed specimens of *Cibicidoides* were analyzed from the >150 μm size fraction because of the relative paucity of benthic foraminifers in some intervals. The benthic isotope record is near continuous except for part of MIS 7 where benthic foraminifers are very rare owing to disso-

lution. Details of analytical methods and tabulation of stable isotope results are available in a data report that is available electronically at www.odp-tamu.edu/publications/177_SR/177TOC.HTM [Hodell *et al.*, 2002].

4. Results

[12] Oxygen isotopes of benthic foraminifers were used to correlate each record to a common timescale (Figure 4a). Despite large differences in sedimentation rates, the amplitudes of the glacial-to-interglacial benthic $\delta^{18}\text{O}$ signals are fairly



similar for the past 1.1 Ma. The range in benthic $\delta^{18}\text{O}$ values at Site 1088 is slightly less than the other records, but even this low sedimentation rate site captures most of the glacial-to-interglacial $\delta^{18}\text{O}$ signal. For example, Site 1088 shows a $\delta^{18}\text{O}$ range of 1.6‰ between the last glaciation and Holocene, which includes a glacial-to-interglacial ice volume effect (up to 1.2‰) and cooling of mid-depth waters (0.4‰). The details of the age models presented here are not definitive and could be subject to refinement in the future. Of course, the precision in correlation is no better than the sampling resolution of the core with the lowest sedimentation rate (Site 1088) and, therefore, we restrict our consideration of vertical gradients to the first-order glacial/interglacial features.

[13] Unlike the generally similar amplitudes of the benthic $\delta^{18}\text{O}$ signals, the benthic $\delta^{13}\text{C}$ records are distinctly offset from one another. Benthic $\delta^{13}\text{C}$ values at Site 1088 are always greater than those at either Site 1090 or 1089, and the magnitude of glacial-to-interglacial $\delta^{13}\text{C}$ variation is small at Site 1088 compared to the deeper records (Figure 4b). This reduced benthic $\delta^{13}\text{C}$ amplitude at Site 1088 cannot be attributed to lower sedimentation rates because the benthic $\delta^{18}\text{O}$ record captures nearly the full glacial-to-interglacial signal. Furthermore, the planktic $\delta^{13}\text{C}$ signals of *G. bulloides* are nearly identical between Sites 1088 and 1090, which suggests that the differences in benthic $\delta^{13}\text{C}$ must be genuine (Figure 5a). The benthic $\delta^{13}\text{C}$ signal at Site 1088 is also consistent with other mid-depth South Atlantic $\delta^{13}\text{C}$ records such as piston core TTN057-20 (1312 m) on the Discovery Seamount for the last 20 kyrs [Ninnemann and Charles, 2002], and with Site 1087A (1372 m) for the last 400 kyrs, which was drilled in the Southern Cape Basin off South Africa [Pierre et al., 2001]. Both these sites are at intermediate water depth and influenced by upper CDW and Antarctic Intermediate Water (AAIW).

[14] At Site 1090, we measured both *C. wuellerstorfi* and *C. kullenbergi* to test if $\delta^{13}\text{C}$ differences existed between these species. Hodell et al. [2001a] reported that paired analyses of these species from the same samples had a 1:1 corre-

spondence for $\delta^{18}\text{O}$, but $\delta^{13}\text{C}$ of *C. kullenbergi* diverged from *C. wuellerstorfi* at lower $\delta^{13}\text{C}$ values suggesting that *C. kullenbergi* may sometimes live infaunally. At Site 1090, *C. kullenbergi* is abundant during interglacial stages but is rare during glacial periods. For discrete points during the glacial episodes, $\delta^{13}\text{C}$ values of *C. wuellerstorfi* were as much as 0.6‰ greater than *C. kullenbergi* (Figure 4b). For the last glacial period, the $\delta^{13}\text{C}$ values of *C. kullenbergi* at Site 1090 are nearly identical to *Cibicides* spp. at Site 1089 [Ninnemann et al., 1999], whereas $\delta^{13}\text{C}$ values of *C. wuellerstorfi* at Site 1090 are clearly greater than *Cibicides* spp. at Site 1089. There is also a slight difference between $\delta^{13}\text{C}$ values of *C. wuellerstorfi* at Site 1090 and *C. kullenbergi* and at *Cibicides* spp. Sites 1090 and 1089, respectively, in the latter part of MIS6. For the remainder of the record, the $\delta^{13}\text{C}$ of *C. wuellerstorfi* at Site 1090 is nearly identical to the *Cibicides* spp. record at Site 1089. Regardless of any interspecies discrepancies, the difference in *C. wuellerstorfi* $\delta^{13}\text{C}$ values between the interglacial and glacial periods is still substantially greater at deep Site 1090 than at mid-depth Site 1088.

[15] We reconstructed the vertical $\delta^{13}\text{C}$ gradient between mid-depth (2082 m) and deep (3702 m) waters by subtracting $\delta^{13}\text{C}$ values at Site 1088 from those at Site 1090 for the last 1.1 Ma (Figure 6). We used the Site 1090 record to calculate the gradient as opposed to the Site 1089 record because: (1) *C. wuellerstorfi* and *C. kullenbergi* were analyzed separately at Site 1090, whereas they were combined at Site 1089; (2) the Site 1090 record is longer than Site 1089 and the $\Delta^{13}\text{C}$ gradient with Site 1088 can be calculated for the last 1.1 myr; and (3) the sedimentation rates at Site 1090 (3 cm/1000 yr) are closer to those at Site 1088 (1 cm/1000 yr) than they are at Site 1089 (15 cm/1000 yr). To calculate the $\Delta^{13}\text{C}$ gradient, carbon isotopic signals were interpolated to provide a constant sampling of 5 kyrs, which matches the sampling interval of the lowest resolution record (Site 1088). The intermediate-to-deep carbon isotopic gradient ($\Delta^{13}\text{C}_{\text{I-D}}$) approaches zero during most interglacial stages of the last 600 kyrs and increases to -1 to -1.5 ‰

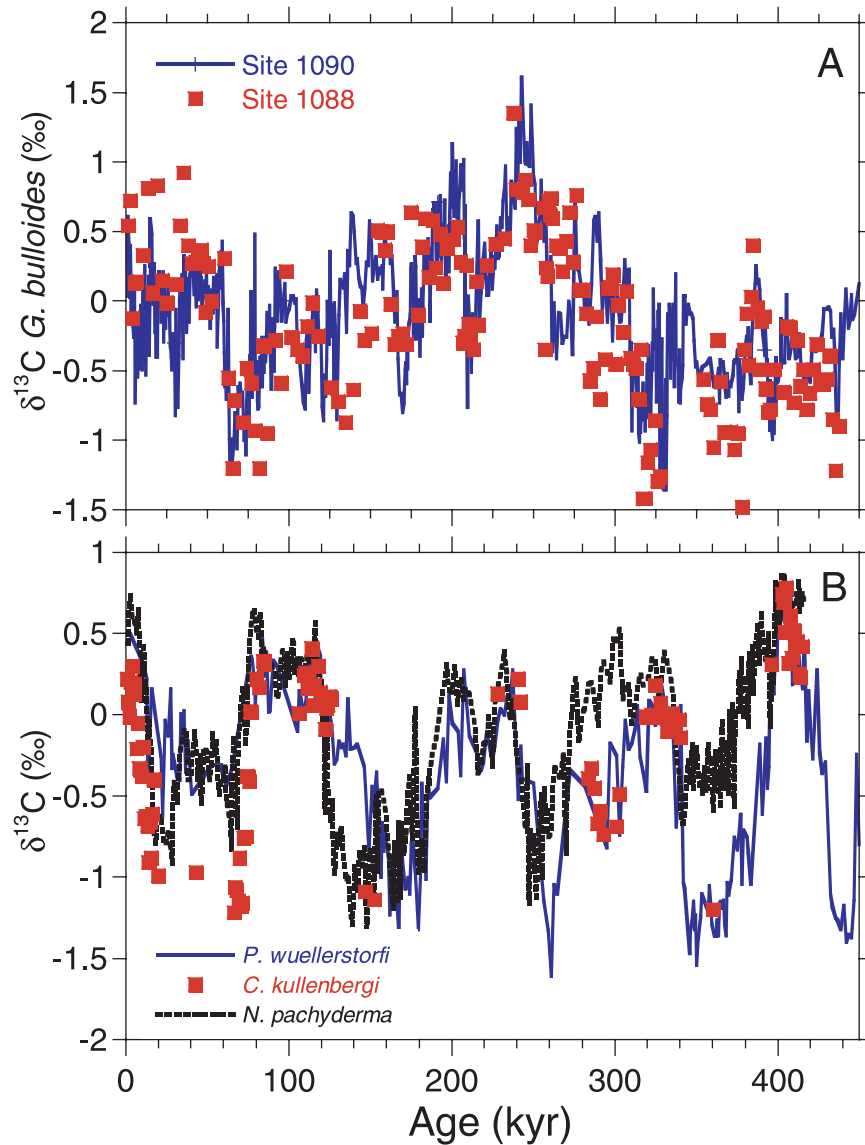


Figure 5. (a) Carbon isotope records of the planktic foraminifer *Globigerina bulloides* at Sites 1090 (solid blue line) and 1088 (filled red squares). (b) Comparison of benthic $\delta^{13}\text{C}$ records of *C. wuellerstorfi* (blue line) and *C. kullenbergi* (filled red squares) and the planktic $\delta^{13}\text{C}$ signal of *N. pachyderma* (dashed black line) at Site 1090.

during glacial stages (Figure 6). For the last 600 kyrs, $\Delta^{13}\text{C}_{\text{I-D}}$ variations are marked by a strong 100-kyr cycle, whereas the pattern is more irregular in the early Pleistocene. The greatest $\Delta^{13}\text{C}_{\text{I-D}}$ values of -1.5‰ occur in MIS14 and are followed by a steady trend thereafter toward reduced $\Delta^{13}\text{C}_{\text{I-D}}$ during glaciations from ~ 550 kyrs to 20 kyrs. If $\delta^{13}\text{C}$ values of *C. kullenbergi* are used instead of *P. wuellerstorfi* for the last glaciation at Site 1090, the magnitude of the $\Delta^{13}\text{C}$ gradient is increased and comparable to those that would be

obtained if the Site 1089 $\delta^{13}\text{C}$ signal were used as the deep-water site.

[16] Weight percent carbonate (wt.% CaCO_3) was measured along the depth transect down the northern flank of the Agulhas Ridge [Hodell *et al.*, 2001b]. Carbonate variations at Site 1088 (2082 m) were negligible as this site has always been above the lysocline (Figure 7). Wt.% CaCO_3 at Site 1090 (3702 m) fluctuates between those at shallower Site 1088 (2082 m) and deeper Site 1089

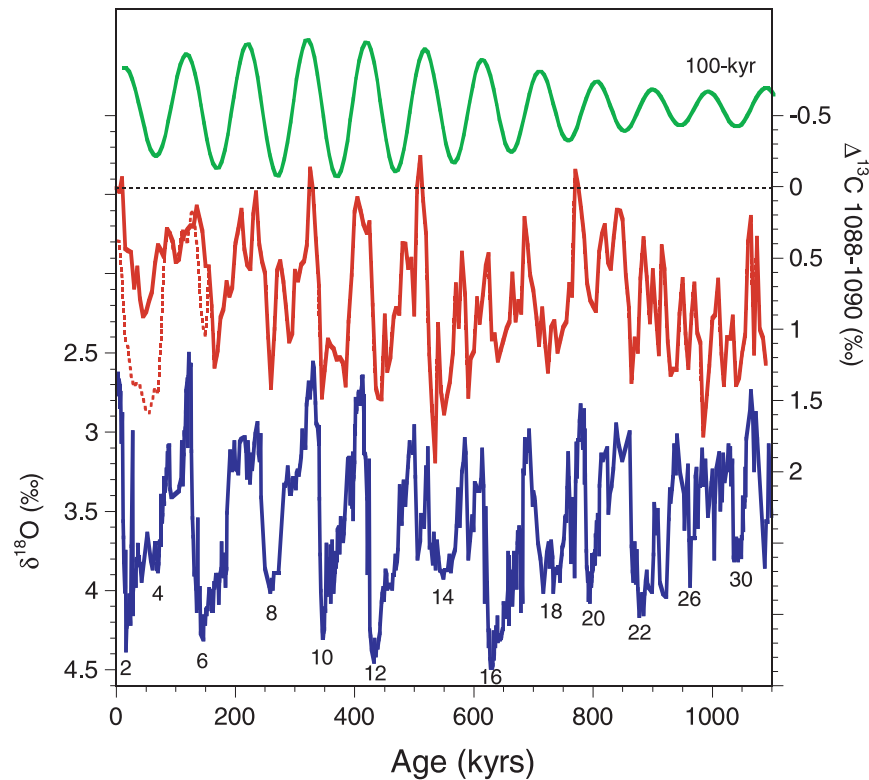


Figure 6. (bottom) Benthic oxygen isotope stratigraphy at Site 1090 (blue line) with designated marine isotope stages. (center) Benthic carbon isotope gradient between mid-depth Site 1088 (2082 m) and deep Site 1090 (3702 m). Solid red line is based on *C. wuellerstorfi* $\delta^{13}\text{C}$ data only at Sites 1090 and 1088. Dashed red line represents the gradient obtained using *C. kullenbergi* at Site 1090 and *C. wuellerstorfi* at Site 1088 (top) Filtered 100-kyr component of the $\Delta^{13}\text{C}$ (1088–1090) gradient (green line).

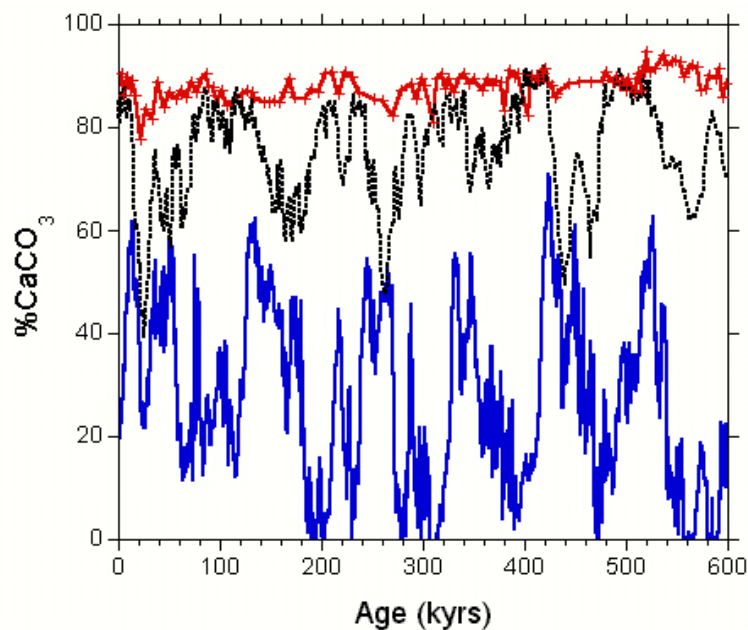


Figure 7. Weight percent carbonate records from Sites 1088 (2082 m, red line), 1090 (3702 m, black line), and 1089 (4621 m, blue line) along a depth transect in the southernmost Cape Basin.



(4620 m), approaching values at Site 1088 during interglacial periods and decreasing toward Site 1089 during glacials.

5. Discussion

5.1. Controls on Benthic $\delta^{13}\text{C}$

[17] Variations in benthic $\delta^{13}\text{C}$ can be caused by several factors including changes in nutrient distribution, air-sea exchange, and potential artifacts such as the “phytodetritus effect” [Mackensen *et al.*, 1993]. In the last glacial ocean, it is estimated that the $\delta^{13}\text{C}$ of the whole ocean decreased by 0.32‰ (relative to the Holocene) [Duplessy *et al.*, 1988; Boyle, 1992]. This is the same magnitude of $\delta^{13}\text{C}$ change observed at Site 1088 between the last glaciation and Holocene (Figure 4b), suggesting that ventilation of mid-depth waters in the South Atlantic was similar to today. Below 2500 m, $\delta^{13}\text{C}$ values decreased markedly during glaciations, indicating that deep water was either more nutrient-rich and/or less well ventilated than today. A problem with interpreting decreased glacial $\delta^{13}\text{C}$ in terms of elevated nutrient concentrations is that Cd/Ca of benthic foraminifera remained unchanged between glacial and interglacial periods [Boyle and Rosenthal, 1996, and references therein]. The $\delta^{13}\text{C}$ -Cd discrepancy can be partly explained if low glacial benthic $\delta^{13}\text{C}$ values in the Southern Ocean did not entirely represent nutrient changes, but rather were related to reduced air-sea exchange [Broecker and Maier-Reimer, 1992; Broecker, 1993]. Foraminiferal Cd/Ca is not without its complications, however, and can be influenced by dissolution at water depths below 2.5 km [McCorkle *et al.*, 1995].

[18] Likewise, the $\delta^{13}\text{C}$ of benthic foraminifera may not always reflect bottom water DIC because of the decomposition of ^{13}C -depleted organic matter that creates a low $\delta^{13}\text{C}$ microhabitat [Mackensen *et al.*, 2001]. Because our sites are separated by less than 2° of latitude, it is unlikely that they experienced dramatically different changes in productivity or organic matter rain rates. Nonetheless, it is still possible that differences in deep water current velocity among sites affected the accumulation of phyto-detritus. For example, sediments at the crest of the Agulhas Ridge are winnowed by

strong currents that may have prevented the accumulation of a phyto-detritus layer at shallow Sites 1088. In contrast, the more quiescent environments of deep Sites 1089 and 1090 may have been more conducive to development of a phyto-detritus layer. Although we cannot rule out a phyto-detritus effect on our records, the differences between the $\delta^{13}\text{C}$ records of Site 1088 and the deeper sites are large, and cannot be explained by a 0.3–0.4‰ correction that has been proposed for productivity-induced changes in benthic $\delta^{13}\text{C}$ during the last glaciation [Mackensen *et al.*, 2001].

[19] In addition, the large glacial-to-interglacial changes observed in benthic $\delta^{13}\text{C}$ at Site 1090/TTN057-6 are also mirrored in the planktic $\delta^{13}\text{C}$ signal of *Neogloboquadrina pachyderma* and, to a lesser extent, in the $\delta^{13}\text{C}$ of *G. bulloides* (Figure 5b). It is difficult to understand how the deep benthic (4600 and 3700 m) and shallow planktic records in the southern Cape Basin can display such large variations in $\delta^{13}\text{C}$, yet the mid-water depth benthic signal at 2100 m shows much smaller amplitude changes. This implies that a mid-depth water mass with small glacial-to-interglacial changes in $\delta^{13}\text{C}$ is sandwiched between deepwater and surface water with large $\delta^{13}\text{C}$ variations. The source area for mid-depth water in the glacial South Atlantic must have been different from Southern Ocean deep water and Subantarctic Surface Water.

5.2. Comparison of Site 1088 With North Atlantic and Pacific Records

[20] One of the most puzzling features of deep benthic $\delta^{13}\text{C}$ records from the Southern Ocean is that values during glacial periods are often less than those in the deep Pacific [Oppo *et al.*, 1990; Venz and Hodell, 2002]. This is not the case for mid-depth water, however, because at no time during the Pleistocene do benthic $\delta^{13}\text{C}$ values at Site 1088 fall below those of deep Pacific Site 849 (Figure 8). In fact, the benthic $\delta^{13}\text{C}$ variations at Site 1088 parallel those at Sites 552 and 849, but absolute $\delta^{13}\text{C}$ values at Site 1088 remain intermediate between the North Atlantic and Pacific end-members. In contrast to mid-depth Site 1088, benthic $\delta^{13}\text{C}$ values at deep sites 1089 and 1090

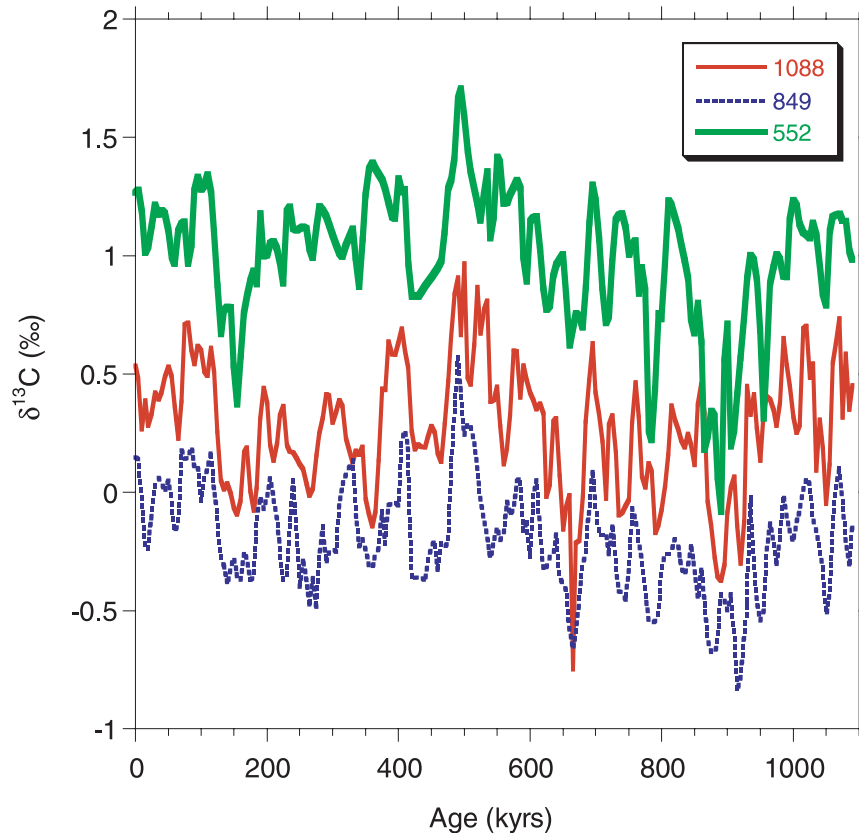


Figure 8. Comparison of benthic $\delta^{13}\text{C}$ records from the mid-depth North Atlantic (Site 522, 2200 m, green line), mid-depth South Atlantic (Site 1088, 2082 m, red line), and deep Pacific (Site 849, 3850 m, dashed blue line). Note that $\delta^{13}\text{C}$ variations at Site 1088 are similar to the other sites, and values are always intermediate between those of the North Atlantic and Pacific end-members.

were up to 1‰ lower than Pacific Site 849 during each glacial of the last 1.1 Ma (Figure 9). Even if one applied a $\delta^{13}\text{C}$ correction of 0.3 to 0.4‰ to allow for a “phytodetritus effect” [Mackensen *et al.*, 2001] the reversed gradient between the South Atlantic and Pacific would not be eliminated.

[21] Our data clearly demonstrate that the Pleistocene carbon isotope signal of mid-depth water evolved differently than deep waters in the South Atlantic. Several potential source areas exist for this well-ventilated, glacial mid-depth water in the South Atlantic. During glacials, production of lower NADW was reduced and GNAIW (also referred to as upper NADW) was enhanced [Oppo and Lehman, 1993]. Opinions vary widely, however, as to how much influence GNAIW had on global circulation [Yu *et al.*, 1996; Oppo and Horowitz, 2000; Matsumoto and Lynch-Steiglitz, 1999]. GNAIW is a candidate for the source of well-ventilated, mid-

depth water to the South Atlantic, but other source areas are also plausible.

[22] The benthic $\delta^{13}\text{C}$ signal amplitude from the mid-depth South Atlantic is similar in amplitude to the planktic $\delta^{13}\text{C}$ record of *N. pachyderma* from piston core E33-22 at 55°S in the Pacific, but is very different from the planktic $\delta^{13}\text{C}$ record of *N. pachyderma* from the subantarctic South Atlantic (Figure 10). The large glacial-to-interglacial $\delta^{13}\text{C}$ changes in subantarctic South Atlantic surface water are not observed in the benthic $\delta^{13}\text{C}$ of intermediate to mid-water depths in the South Atlantic [Ninnemann and Charles, 1997]. Subantarctic surface waters in the southeast Pacific sector of the Southern Ocean may have been a potential source of mid-depth water to the South Atlantic during glacials via the production of Subantarctic Mode Water (SAMW) and transport through the Drake Passage. SAMW is produced in the south-

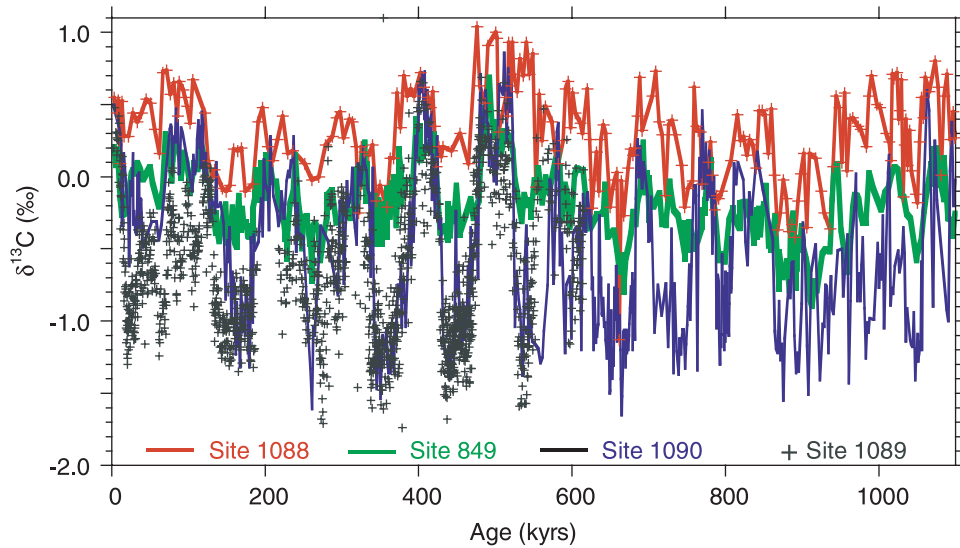


Figure 9. Comparison of benthic $\delta^{13}\text{C}$ records from South Atlantic Sites 1088 (2082 m, red line), 1090 (3702 m, blue line), and 1089 (4621 m, black crosses) and deep Pacific Site 849 (3850 m; green line). Note that $\delta^{13}\text{C}$ values at Site 1088 are never lower than the Pacific, whereas glacial $\delta^{13}\text{C}$ values at the deeper sites (1090 and 1089) are almost always less than the Pacific.

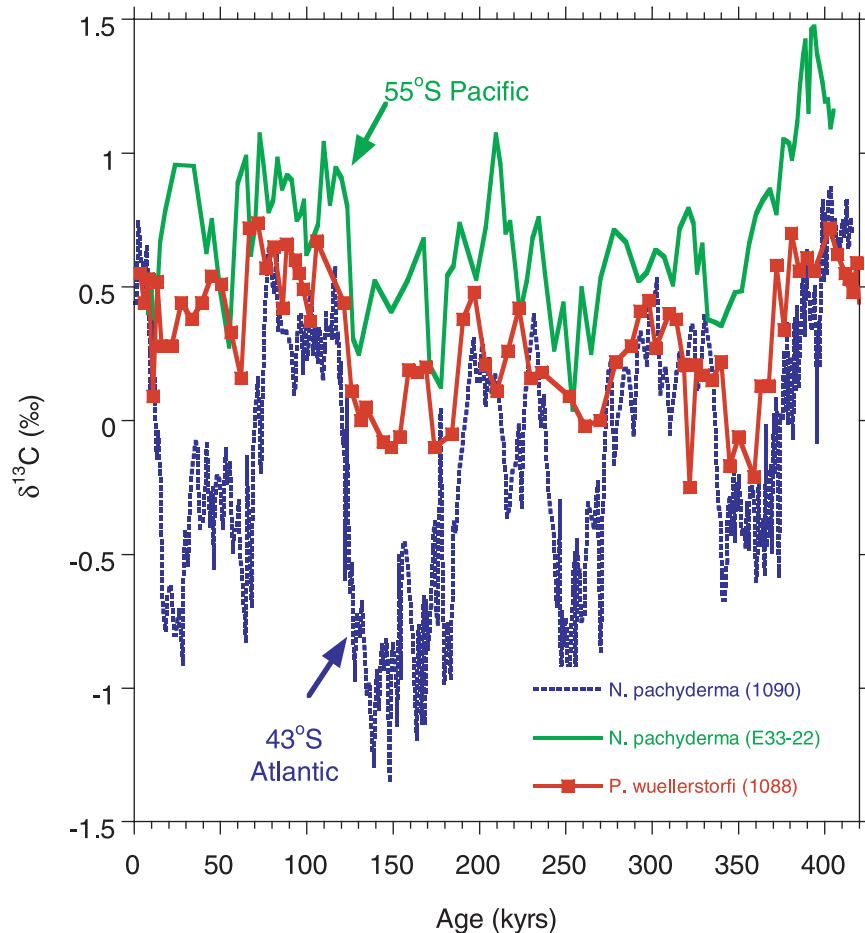


Figure 10. The benthic $\delta^{13}\text{C}$ record from mid-depth Site 1088 (red line) compared to planktic $\delta^{13}\text{C}$ records from South Atlantic Site 1090 (blue dashed line) and South Pacific piston core E33-22 (green line).



Table 2. Holocene and Glacial $\delta^{13}\text{C}$ Values Used in Figure 11

Core	Water Depth, m	$\delta^{13}\text{C}$ Holocene	$\delta^{13}\text{C}$ Glacial	Reference
TTN57-20	1335	0.58	0.38	<i>Ninnemann and Charles</i> [2002]
Site 1087	1372	0.58	0.39	<i>Pierre et al.</i> [2001]
Site 1088	2082	0.5	0.28	this study
PS1754-1	2519	0.59	-0.33	<i>Mackensen et al.</i> [2001]
RC15-93	2714	0.29	-0.96	<i>Ninnemann and Charles</i> [2002]
PS2564-3	3034	0.49	-0.83	<i>Mackensen et al.</i> [2001]
PS2495-3	3134	0.71	-0.42	<i>Mackensen et al.</i> [2001]
PS2499-5	3175	0.31	-0.82	<i>Mackensen et al.</i> [2001]
Site 1090	3702	0.49 (wuel)	-0.30 (wuel)	this study
Site 1090	3702	0.21 (kull)	-1.00 (kull)	this study
TTN057-15	3744	-0.02	-0.81	<i>Ninnemann and Charles</i> [2002]
RC15-94	3762	-0.18	-0.78	<i>Ninnemann and Charles</i> [2002]
PS2498-1	3783	0.22	-1.09	<i>Mackensen et al.</i> [2001]
V22-108	4171	0.12	-0.83	<i>Ninnemann and Charles</i> [2002]
Site 1089	4621	0.3	-1.2	this study
PS2082-1	4661	0.21	-0.79	<i>Mackensen et al.</i> [2001]
RC11-83	4718	0.22	-0.91	<i>Ninnemann and Charles</i> [2002]
TTN057-21	4981	0.27	-0.83	<i>Ninnemann and Charles</i> [2002]

eastern Pacific today by vertical convection along the subantarctic convergence [McCartney, 1977]. Ribbe [2001] proposed that the production of intermediate water in the Southern Ocean is related to the strength Southern Hemisphere winds. Increased wind speeds during glacial periods may have increased the depth of vertical convection in the subantarctic South Pacific, thereby enhancing production of SAMW.

5.3. Intermediate to Deep $\delta^{13}\text{C}$ Gradients ($\Delta^{13}\text{C}_{I-D}$)

[23] For the last glaciation, *Ninnemann and Charles* [2002] reported a sharp increase in the vertical $\delta^{13}\text{C}$ gradient in the South Atlantic between 1335 and 2714 m. We added new data from Sites 1087 [Pierre et al., 2001], 1088, 1089, and 1090 (this study) to their reconstruction along with results from other deep piston cores (>2500 m) from the subantarctic Atlantic Ocean [Mackensen et al., 2001] (Table 2; Figure 11). During the Holocene, intermediate-to-deep $\delta^{13}\text{C}$ gradients were subtle averaging $\sim 0.3\text{‰}$. In contrast, vertical $\delta^{13}\text{C}$ gradients were considerably greater during the last glaciation with a sharp break between 2100 and 2500 m. At sites shallower than 2100 m, the difference in carbon isotopic values between the

last glaciation and Holocene is $\sim 0.3\text{‰}$, which equals the estimated whole-ocean change due to increased nutrient inventories [Duplessy et al., 1988; Boyle, 1992]. At sites below 2500 m, the $\delta^{13}\text{C}$ difference between the last glaciation and Holocene was as high as 1.3‰.

[24] We infer that well-ventilated water extended to a depth of at least 2100 m in the South Atlantic Ocean during the last glaciation. Below ~ 2500 m, glacial deep waters of the South Atlantic were poorly ventilated and significantly depleted in $\delta^{13}\text{C}$ relative to waters above. The sharp carbon isotopic gradient between ~ 2100 and 2500 m supports the existence of a chemical divide between mid-depth and deep waters in the glacial Southern Ocean. This circulation contrasts with the Holocene when both deep and intermediate water were well ventilated (Figure 11) as North Atlantic Deep Water penetrated far into the South Atlantic, altering the physical and chemical properties of Circumpolar Deep Water [Charles and Fairbanks, 1990].

[25] The pattern observed for the last glaciation is reproduced for most glacial stages of the last 1.1 myr (Figure 6), indicating a consistent response of mid-depth and deep water masses in the South Atlantic. During late Pleistocene glacial periods, the deep South Atlantic was filled by a ^{13}C -

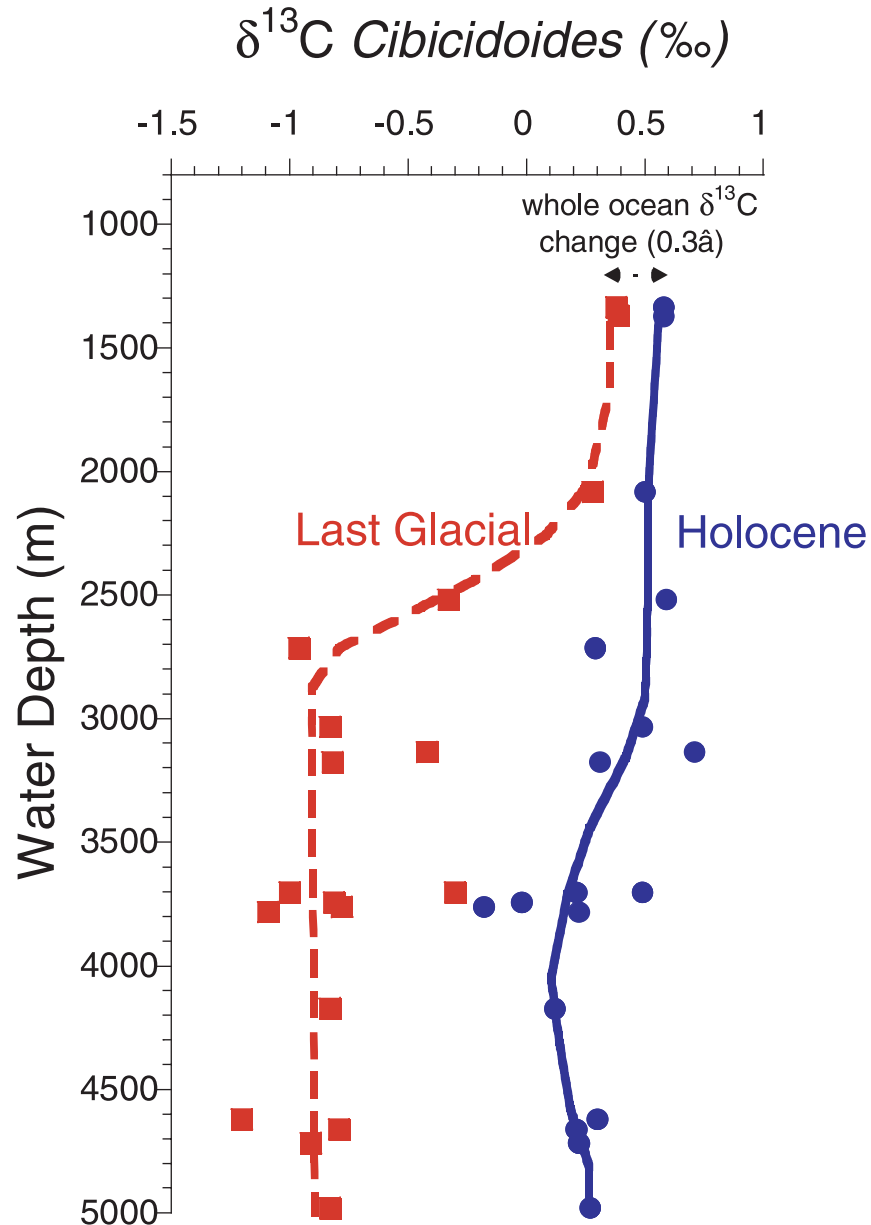


Figure 11. Reconstruction of vertical $\delta^{13}\text{C}$ gradients in the South Atlantic for the Holocene (solid blue line) and last glacial maximum (dashed red line). Data and sources provided in Table 2.

depleted water mass to a depth of ~ 2500 m (Figure 12a). During interglacials, relatively high $\delta^{13}\text{C}$ values extended to depths of >4600 m. The increase in $\Delta^{13}\text{C}_{\text{I-D}}$ in the South Atlantic during glacial periods is similar to that observed in the North Atlantic [Boyle, 1992; Oppo and Lehman, 1993] and Indo-Pacific Ocean [Mix et al., 1991; Herguera et al., 1992; McCorkle et al., 1998; Matsumoto et al., 2002], but the magnitude of

the gradient is substantially greater in the South Atlantic sector of the Southern Ocean than other ocean basins.

5.4. $\Delta^{13}\text{C}_{\text{I-D}}$ and Carbonate Compensation

[26] Pleistocene changes in vertical $\Delta^{13}\text{C}_{\text{I-D}}$ gradients should result in a change in saturation state of deep waters, which is followed by carbonate

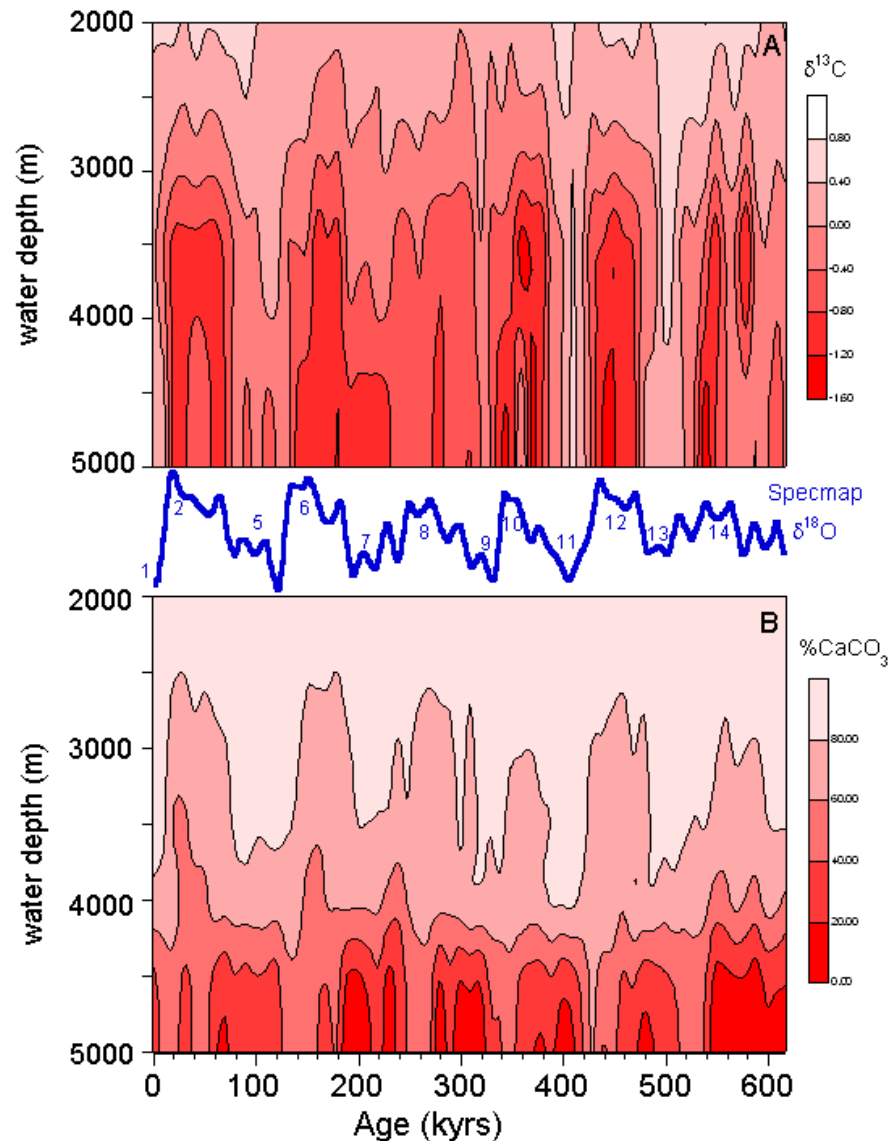


Figure 12. (a) Contoured benthic $\delta^{13}\text{C}$ as a function of water depth and time in the South Atlantic. (b) Contoured weight percent carbonate as a function of water depth and time in the South Atlantic. The Specmap $\delta^{18}\text{O}$ record (blue line) is shown for reference.

compensation as the CCD adjusts to maintain alkalinity balance between riverine input and marine burial [Boyle, 1988]. As $\Delta^{13}\text{C}_{\text{I-D}}$ increases at the start of a glacial cycle, dissolution should increase in deep water as CO_2 is transferred from intermediate to deep water. After several thousands of years, low carbonate ion concentrations in deep water will be “compensated for” by a rise in the CCD resulting in an increase in carbonate saturation during the late glacial period. When $\Delta^{13}\text{C}_{\text{I-D}}$

decreases at a glacial termination, carbonate saturation increase in deep water as CO_2 is redistributed out of the deep ocean into the atmosphere, upper ocean, and mid-depth waters. Oceanic alkalinity then adjusts by a rise in the CCD that increases dissolution in deep water during interglacial periods.

[27] The relation between vertical chemical fraction and carbonate saturation can be examined by

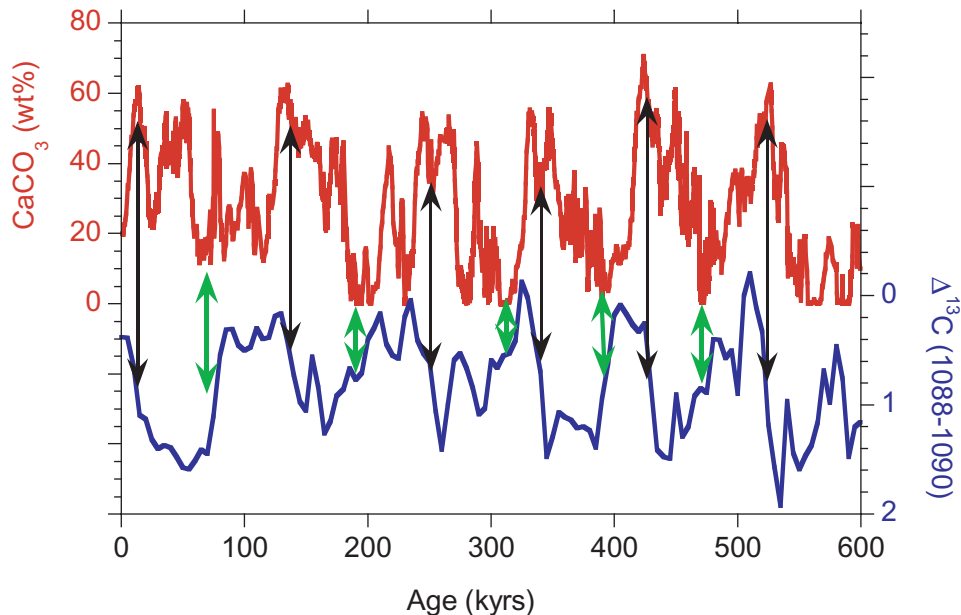


Figure 13. Weight percent carbonate at Site 1089 (red line), reflecting changes in the carbonate saturation state of the deep ocean [Hodell *et al.*, 2001b], compared to the carbon isotopic gradient between mid-depth and deep waters ($\Delta^{13}\text{C}$ 1088–1090, blue line). The carbonate record is in-phase with the first derivative of the $\Delta^{13}\text{C}$ (1088–1090) signal. Black arrows indicate glacial terminations and are marked by a preservation spikes as the vertical $\Delta^{13}\text{C}$ gradient decreases. Green arrows indicate the start of glacial cycles when $\Delta^{13}\text{C}$ (1088–1090) increases and carbonate saturation is low.

comparing $\Delta^{13}\text{C}_{\text{I-D}}$ with the carbonate record from Site 1089 (Figure 13). Percent carbonate variations at Site 1089 (4620 m) represent a qualitative, high-resolution signal of the temporal evolution of the carbonate saturation state of the deep sea [Hodell *et al.*, 2001b]. The carbonate signal is in-phase with the first derivative of the $\Delta^{13}\text{C}_{\text{I-D}}$ record such that each of the decreases in $\Delta^{13}\text{C}_{\text{I-D}}$ at terminations is marked by a carbonate preservation spike followed by increased dissolution during interglacial periods. Similarly, most of the increases in $\Delta^{13}\text{C}_{\text{I-D}}$ at the initiation of glacial cycles are marked by low carbonate values (dissolution), and are followed by increasing carbonate concentrations into the late glacial as carbonate compensation occurs. This pattern of carbonate variation is consistent with that predicted for the response of carbonate dissolution cycles to vertical chemical fractionation [Boyle, 1988]. It is also consistent with the model of Toggweiler [1999] where carbonate ion concentrations below the chemical divide initially decrease at the start of a glacial cycle, followed by carbonate compensation that accounts for ~ 36

ppm drop in CO_2 during the reduced ventilation state.

5.5. Implications for Atmospheric CO_2

[28] Our results are relevant to the “chemical divide” model [Toggweiler, 1999], which ascribes reduced atmospheric pCO_2 during glacial periods to three effects: (1) 21 ppm by reduced ventilation of deep water; (2) 36 ppm due to carbonate compensation; and (3) 23 ppm from decreased surface temperatures. We discuss the relevance of our results to reduced ventilation and carbonate compensation separately because the response time of CO_2 change to each mechanism differs. A unique feature of the “chemical divide” model is that it produces a substantial depletion in glacial benthic $\delta^{13}\text{C}$ values (0.6‰) by reducing ventilation of deep water with minimal change in nutrient content. This mechanism may aid in explaining the discrepancy between Cd and $\delta^{13}\text{C}$ paleotracers. Reduced deep-water ventilation is attributed to a physical process that decreases the vertical exchange between deep

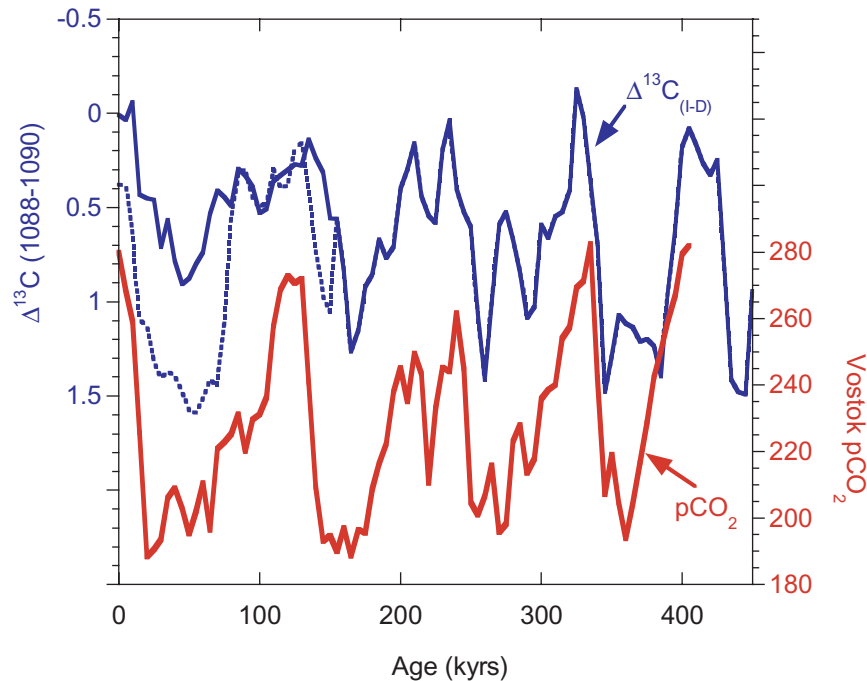


Figure 14. Changes in vertical carbon isotope gradients (blue line) in the South Atlantic compared to $p\text{CO}_2$ variation (red line) in the Vostok ice core. Dotted blue line represents the $\Delta^{13}\text{C}$ gradient obtained using *C. kullenbergi* data at Site 1090 and solid blue line represents *C. wuellerstorfi* data only.

and Antarctic surface waters. Alternatively, *Stephens and Keeling* [2000] have emphasized the role of Antarctic sea ice cover and/or ice-induced stratification for decreasing ventilation rates during glacial periods by limiting air-sea gas exchange. Regardless of causal mechanism, changes in ventilation of Southern Ocean deep water can produce substantial changes in atmospheric CO_2 .

[29] To assess whether changes in vertical chemical gradients in the Southern Ocean may have contributed to atmospheric CO_2 variation [Toggweiler, 1999], we follow the lead of *Oppo and Fairbanks* [1990] and *Flower et al.* [2000] and compare $\Delta^{13}\text{C}_{\text{I-D}}$ (1088–1090) with the $p\text{CO}_2$ in the Vostok ice core (Figure 14) using the astronomically tuned timescale of *Shackleton* [2000]. The curves closely parallel one another but the amplitudes of the signals differ for the last 150 kyrs. A considerably better match is obtained if the $\delta^{13}\text{C}$ data of *C. kullenbergi* at Site 1090 are used in place of *P. wuellerstorfi* for the last 150 kyrs. This is essentially equivalent to using the benthic $\delta^{13}\text{C}$ data of deep Site 1089 in place of 1090 to calculate $\Delta^{13}\text{C}_{\text{I-D}}$ (Figure 4b). The cross correlation coefficient (r)

for the two records is -0.68 with no lag. The signals are coherent at 95% confidence limits for the 100-kyr period only and the phase is -178° (± 9.9), which indicates no detectable lag between $\Delta^{13}\text{C}_{\text{I-D}}$ and atmospheric $p\text{CO}_2$ within the chronological resolution of the $\Delta^{13}\text{C}_{\text{I-D}}$ signal (~ 5 kyrs). A more detailed comparison of the Site 1089 isotopic and Vostok ice core records also found that benthic $\delta^{13}\text{C}$ changes in Site 1089 were essentially synchronous with changes in atmospheric $p\text{CO}_2$ (Mortyn et al., manuscript in preparation, 2002). These results suggest that changes in ventilation rates of Southern Ocean deep water remain a viable mechanism for explaining atmospheric $p\text{CO}_2$ variation.

[30] Atmospheric $p\text{CO}_2$ reduction in Toggweiler's model results both from decreased ventilation and a carbonate alkalinity response to vertical chemical fractionation. Changes in carbonate compensation cannot explain the rapid changes in $p\text{CO}_2$ that occur at terminations because of the lag of the marine carbonate system. Rather, carbonate compensation acts to reinforce $p\text{CO}_2$ changes that are caused by other mechanisms (sea ice, ventilation,



nutrient changes, etc.) [Broecker and Peng, 1987]. Hodell et al. [2001b] demonstrated how carbonate compensation may control some of the second-order features in the pCO₂ curve from ice cores. For example, the rise of pCO₂ during the Holocene may be the result of a compensation response of the carbonate system to oceanic redistribution of alkalinity and DIC during the last deglaciation [Broecker et al., 1999].

5.6. Implications for the Mid-Pleistocene Climate Transition

[31] By partitioning the ice volume and temperature effects in the benthic δ¹⁸O signal using the δ¹⁸O of O₂ in the Vostok ice core, Shackleton [2000] demonstrated that ice-volume component of δ¹⁸O lags eccentricity. Consequently, the 100-kyr signal in paleoclimate records cannot be the result of ice volume changes; instead, Shackleton [2000] advocated the 100-k cycle may be produced by changing atmospheric pCO₂. A strong 100-kyr cycle emerged in paleoclimate records in the middle Pleistocene during the so-called Mid-Pleistocene Revolution (MPR [Berger and Jansen, 1994]). The traditional view is that the pacing of the 100-kyr cycle was due to the development of large ice sheets, which act as an internal oscillator with a long time constant [Clark et al., 1999]. If the 100-kyr cycle was not set by ice volume [Shackleton, 2000], or the dynamics of large ice sheets, then perhaps the MPT was driven by the Earth's carbon cycle.

[32] A high degree of correlation has been noted between Atlantic Δ¹³C_{I-D} and atmospheric pCO₂ by others [Oppo and Fairbanks, 1990; Flower et al., 2000]. Although this match does not necessarily prove a causal link, we examined how Δ¹³C_{I-D} changed in the Southern Ocean during the mid-Pleistocene and whether it is consistent with CO₂-forcing during the MPR. The observed mid-Pleistocene increase of the 100-kyr cycle in Δ¹³C_{I-D} (Figure 6) supports a change in vertical fractionation and deep-water ventilation rates in the Southern Ocean [Raymo et al., 1997]. To the extent that Δ¹³C_{I-D} was correlated with pCO₂ in the middle Pleistocene, then CO₂-forcing and, implic-

itly, the ventilation of the deep ocean may have been important during the MPR.

6. Conclusion

[33] Using a depth transect of benthic δ¹³C records down the northern flank of the Agulhas Ridge in the South Atlantic, we show that the carbon isotopic signal of mid-depth waters evolved differently from deep waters during the Pleistocene. Unlike the deeper sites, glacial benthic δ¹³C values at mid-depth Site 1088 (2100 m) never fall below those of the Pacific at anytime during the last 1.1 myr. The intermediate-to-deep δ¹³C gradient (Δ¹³C_{I-D}) increased markedly during each glacial stage and approached zero during most interglacials. Our results support the existence of a sharp chemocline between ~2100 and 2700 m in the Southern Ocean during Pleistocene glacial periods, which separated well-ventilated waters above 2100 m from poorly-ventilated deep water masses below 2700 m. The Δ¹³C_{I-D} signal parallels late Pleistocene changes in atmospheric pCO₂ over the last four glacial cycles, suggesting that vertical chemical gradients in the Southern Ocean may have contributed to atmospheric pCO₂ variation. During the mid-Pleistocene, the power of the 100-kyr cycle increased progressively in the Δ¹³C_{I-D} signal, which may indicate that changes in Southern Ocean deep-water ventilation played a role in the MPR through its affect on atmospheric pCO₂.

Acknowledgments

[34] We thank J. Curtis for assistance with stable isotope analysis, and R. Toggweiler and J. Lynch-Stieglitz for reviewing the paper and providing valuable suggestions for improvement. The ODP provided samples for this study with sponsorship from the NSF. This research was supported by the US Science Support Program and NSF Grant OCE-99007036.

References

- Berger, W. H., and E. Jansen, Mid-Pleistocene climate shift: The Nansen connection, in *The Polar Oceans and Their Role in Shaping the Global Environment*, Geophys. Monogr. Ser., vol. 85, edited by Johannessen et al., pp. 295–311, AGU, Washington, D. C., 1994.
- Boyle, E. A., The role of vertical chemical fractionation in controlling late Quaternary atmospheric carbon dioxide, *J. Geophys. Res.*, 93, 15,701–15,714, 1988.



- Boyle, E. A., Cd and $\delta^{13}\text{C}$ paleochemical ocean distributions during the stage 2 glacial maximum, *Ann. Rev. Earth Planet. Sci.*, 20, 245–287, 1992.
- Boyle, E. A., and Y. Rosenthal, Chemical hydrography of the South Atlantic during the last glacial maximum: Cd vs. $\delta^{13}\text{C}$, in *The South Atlantic: Present and Past Circulation*, edited by G. Wefer et al., pp. 423–443, Springer-Verlag, New York, 1996.
- Broecker, W. S., An oceanographic explanation for the apparent carbon isotope-cadmium discordancy in the glacial Antarctic?, *Paleoceanography*, 8, 137–139, 1993.
- Broecker, W. S., and E. Maier-Reimer, The influence of air and sea exchange on the carbon isotope distribution in the sea, *Global Biogeochem. Cycles*, 6, 315–320, 1992.
- Broecker, W. S., and T.-H. Peng, The role of CaCO_3 compensation in the glacial to interglacial atmospheric CO_2 change, *Global Biogeochem. Cycles*, 1, 15–19, 1987.
- Broecker, W. S., E. Clark, D. C. McCorkle, T.-H. Peng, I. Hajdas, and G. Bonani, Evidence for a reduction in the carbonate ion content of the deep sea during the course of the Holocene, *Paleoceanography*, 14, 744–752, 1999.
- Charles, C. D., and R. G. Fairbanks, Glacial to interglacial changes in the isotopic gradients of Southern Ocean surface water, in *Geological History of the Polar Oceans: Arctic Versus Antarctic*, edited by U. Bleil and J. Thiede, pp. 519–538, Kluwer Acad., Norwell, Mass., 1990.
- Clark, P. U., R. B. Alley, and D. Pollard, Northern Hemisphere ice-sheet influences on global climate change, *Science*, 286, 1104–1111, 1999.
- Duplessy, J.-C., N. J. Shackleton, R. G. Fairbanks, L. Labeyrie, D. Oppo, and N. Kallel, Deepwater source variations during the last climatic cycle and their impact on the global deep-water circulation, *Paleoceanography*, 3, 343–360, 1988.
- Flower, B. P., D. W. Oppo, K. A. Venz, D. A. Hodell, J. F. McManus, and J. Cullen, North Atlantic intermediate- to deep water circulation and nutrient redistribution during the past 1 m.y., *Paleoceanography*, 15, 388–403, 2000.
- Gersonde, R., et al., *Proc. Ocean Drill. Program Initial Rep.*, vol. 177 [CD-ROM], Ocean Drill. Program, College Station, Tex., 1999.
- Herguera, J. C., E. Jansen, and W. H. Berger, Evidence for a bathyal front at 2000 m depth in the glacial Pacific, based on a depth transect on Ontong Java Plateau, *Paleoceanography*, 7, 273–288, 1992.
- Hodell, D. A., C. D. Charles, and U. S. Ninnemann, Comparison of interglacial stages in the South Atlantic sector of the southern ocean for the past 450 kys: Implications for Marine Isotope Stage (MIS) 11, *Global Planet. Change*, 24, 7–26, 2000.
- Hodell, D. A., J. H. Curtis, F. J. Sierro, and M. E. Raymo, Correlation of late Miocene-to-early Pliocene sequences between the Mediterranean and North Atlantic, *Paleoceanography*, 16, 164–178, 2001a.
- Hodell, D. A., C. D. Charles, and F. J. Sierro, Late Pleistocene evolution of the ocean's carbonate system, *Earth Planet. Sci. Lett.*, 192, 109–124, 2001b.
- Hodell, D. A., C. D. Charles, J. H. Curtis, P. G. Mortyn, U. S. Ninnemann, and K. A. Venz, Data report: Oxygen isotope stratigraphy of ODP Leg 177 Sites 1088, 1089, 1090, 1093, and 1094, *Proc. Ocean Drill. Program Sci. Results*, 177, 2002. (Available at http://www-odp.tamu.edu/publications/177_SR/).
- Kroopnick, P. M., The distribution of ^{13}C in the world oceans, *Deep Sea Res.*, 32, 57–84, 1985.
- Lynch-Stieglitz, J., R. G. Fairbanks, and R. G. Charles, Glacial-interglacial history of Antarctic Intermediate Water: Relative strengths of Antarctic versus Indian Ocean sources, *Paleoceanography*, 9, 7–29, 1994.
- Mackensen, A., H. W. Hubberten, T. Bickert, G. Fischer, and D. K. Fütterer, The $\delta^{13}\text{C}$ in benthic foraminiferal tests of *Fontbotia wuellerstorfi* (Schwager) relative to the $\delta^{13}\text{C}$ of dissolved inorganic carbon in Southern Ocean deep water: Implications for glacial ocean circulation models, *Paleoceanography*, 8, 587–610, 1993.
- Mackensen, A., M. Rudolph, and G. Kuhn, Late Pleistocene deep-water circulation in the subantarctic eastern Atlantic, *Global Planet. Change*, 30, 197–229, 2001.
- Matsumoto, K., and J. Lynch-Stieglitz, Similar glacial and Holocene deep water circulation inferred from southeast Pacific benthic foraminiferal carbon isotope composition, *Paleoceanography*, 14, 149–163, 1999.
- Matsumoto, K., T. Oba, J. Lynch-Stieglitz, and H. Yamamoto, Interior hydrography and circulation of the glacial Pacific Ocean, *Quat. Sci. Rev.*, 21, 1693–1704, 2002.
- McCartney, M. S., Subantarctic Mode water, in *A Voyage of Discovery*, edited by A. Angel, pp. 103–119, Pergamon, New York, 1977.
- McCorkle, D. C., P. M. Martin, D. W. Lea, and G. P. Klunkhammer, Evidence of a dissolution effect on benthic foraminiferal shell chemistry: $\delta^{13}\text{C}$, Cd/Ca, Ba/Ca, and Sr/Ca results from the Ontong Java Plateau, *Paleoceanography*, 10, 699–714, 1995.
- McCorkle, D. C., D. T. Heggie, and H. H. Veeh, Glacial and Holocene stable isotope distributions in the southeastern Indian Ocean, *Paleoceanography*, 13, 20–34, 1998.
- Mix, A. C., N. G. Pisias, R. Zahn, W. Rugh, C. Lopez, and K. Nelson, Carbon 13 in Pacific and intermediate waters, 0–370 ka: Implications for ocean circulation and Pleistocene CO_2 , *Paleoceanography*, 6, 205–226, 1991.
- Ninnemann, U. S., and C. D. Charles, Regional differences in Quaternary Subantarctic nutrient cycling: Link to intermediate and deep water ventilation, *Paleoceanography*, 12, 560–567, 1997.
- Ninnemann, U. S., and C. D. Charles, Changes in the mode of Southern Ocean circulation over the last glacial cycle revealed by foraminiferal stable isotopic variability, *Earth Planet. Sci. Lett.*, 201, 383–396, 2002.
- Ninnemann, U. S., C. D. Charles, and D. A. Hodell, Origin of global millennial scale climate events: constraints from the Southern Ocean deep sea sedimentary record, in *Mechanisms of Global Climate Change at Millennial Time Scales*, *Geophys. Monogr. Ser.*, vol. 112, edited by P. U. Clark, R. S. Webb, and L. D. Keigwin, pp. 99–112, AGU, Washington, D. C., 1999.
- Oppo, D. W., and R. G. Fairbanks, Atlantic Ocean thermohaline circulation of the last 150,000 years: Relationship to climate and atmospheric CO_2 , *Paleoceanography*, 5, 277–288, 1990.



- Oppo, D. W., and M. Horowitz, Glacial deep water geometry: South Atlantic benthic foraminiferal Cd/Ca and $\delta^{13}\text{C}$ evidence, *Paleoceanography*, *15*, 147–160, 2000.
- Oppo, D. W., and S. J. Lehman, Mid-depth circulation of the subpolar North Atlantic during the last glacial maximum, *Science*, *259*, 1148–1152, 1993.
- Oppo, D. W., R. G. Fairbanks, A. L. Gordon, and N. J. Shackleton, Late Pleistocene southern ocean $\delta^{13}\text{C}$ variability, *Paleoceanography*, *5*, 43–54, 1990.
- Pierre, C., J. F. Saliege, M. J. Urrutiaguer, and J. Giraudeau, Stable isotope record of the last 500 k.y. at Site 1087 (Southern Cape Basin), in Proc. of Ocean Drill. Program, Sci. Results, vol. 175, edited by G. Wefer, W. H. Berger, and C. Richter, Ocean Drill. Program, College Station, Tex., 2001. (Available at http://www-odp.tamu.edu/publications/175_SR/chap_12/chap_12.htm).
- Raymo, M. E., D. W. Oppo, and W. Curry, The mid-Pleistocene climate transition: A deep sea carbon isotopic perspective, *Paleoceanography*, *12*, 546–559, 1997.
- Ribbe, J., Intermediate water mass production controlled by Southern Hemisphere winds, *Geophys. Res. Lett.*, *28*, 535–538, 2001.
- Shackleton, N. J., The 100,000-year ice-age cycle identified and found to lag temperature, carbon dioxide, and orbital eccentricity, *Science*, *289*, 1897–1902, 2000.
- Shipboard Scientific Party, Leg 177 summary: Southern Ocean paleoceanography, in *Proc. Ocean Drill. Program Init. Rep.*, *177*, 1–67, 1999.
- Stephens, B. B., and R. F. Keeling, The influence of Antarctic sea ice on glacial-interglacial CO_2 variations, *Nature*, *404*, 171–174, 2000.
- Toggweiler, J. R., Variation of atmospheric CO_2 by ventilation of the ocean's deepest water, *Paleoceanography*, *14*, 571–588, 1999.
- Venz, K. A., and D. A. Hodell, New evidence for changes in Plio-Pleistocene deep water circulation from Southern Ocean ODP Leg 177 Site 1090, Site 1090, *Palaeogeogr. Palaeoclimatol. Palaeoecol.*, *182*, 197–220, 2002.
- Wildeboer Shut, E., G. Uenzelmann-Neben, and R. Gersonde, Seismic evidence for bottom current activity at the Agulhas Ridge, *Global Planet. Change*, *34*, 185–198, 2002.
- Yu, E.-F., R. Francois, and M. P. Bacon, Similar rates of modern and last-glacial ocean thermohaline circulation inferred from radiochemical data, *Nature*, *379*, 689–694, 1996.